JOURNAL OF PROPULSION AND POWER
Vol. 19, No. 2, March–April 2003

Design and Use of a Batch Reactor for Catalytic Decomposition of Propellants

Rachel Eloirdi,* Sylvie Rossignol,† Charles Kappenstein,‡ and Daniel Duprez§
Centre National de la Recherche Scientifique, Université de Poitiers, F-86022 Poitiers, France
and
Nicolas Pillet¶
Centre National d'Etudes Spatiales, F-31401 Toulouse, France

The toxicity of pure hydrazine has prompted the research of possible "green propellants" to replace this monopropellant for small thruster use. To fulfill this objective, a constant volume computerized batch reactor has been developed, which permits study of different monopropellants and their associated catalysts. This reactor can be used as a screening reactor, and its main advantages are easy use, fast change of catalyst or propellant, very limited consumption of propellant or catalyst, and simultaneous recording of reactor pressure, catalyst, and gas-phase temperatures. The catalyst can be preheated, and the working pressure is between vacuum and 2 bars. The main parameters that can be obtained for the catalyst evaluation are the catalytic decomposition rate, the ignition delay, and the onset decomposition temperature. Three propellants have been checked: pure hydrazine, hydrogen peroxide, and a hydroxylammonium nitrate–(HAN–)triethanolammonium nitrate–(TEAN–) water mixture; they display similar rates and ignition delays but the HAN-based propellant needs higher initial temperature and leads to the simultaneous formation of condensed products at low temperature. For a specific propellant, the results lead to a classification of different catalytic beds before further investigations in dynamic reactors using real working conditions.

Introduction

HYDRAZINE is the most common propellant used in chemical propulsion for small thrusters, and the catalytic decomposition is obtained by flowing the propellant through a catalytic bed made of alumina-supported iridium pellets.[1] Recently, several papers focused on the possibility to replace hydrazine by other monopropellant options[2–4] to avoid the disadvantages due to the known toxicity of hydrazine associated with its high vapor pressure at 20°C (14 mbar). Among different possibilities, hydroxylammonium nitrate- (HAN-) based aqueous mixtures appear the most promising, and different reductants have been checked with favorable results, such as triethanolammonium nitrate (TEAN),[5,6] glycine, methanol, and ethanol.[6–8] Concentrated hydrogen peroxide solutions could be another choice, alone[9,10] or associated with polyethylene in a hybrid thruster.[11–14] Each monopropellant composition has to be associated with the best catalytic material, which has to be active and maintain stability under operating conditions. The temperature onset of the catalytic decomposition must be as low as possible to avoid preheating of the catalyst bed at high temperatures.

Most of the experimental work has been performed by using performance evaluation tools working in real conditions (thruster or dynamic reactor); the drawbacks of these experiments are the consumption of large quantities of propellant (of the order of one to several liters) and the amount of the catalyst sample used for the catalytic bed (a few grams to tens of grams). The testing of new propellant formulations, as well as the screening of numerous different catalysts, needs the development of reactors working at the laboratory level, to reduce the cost of the trial runs. Such reactors will be used at conditions less representative than the thruster conditions, but with limited amounts of reactants. A recent paper described one of these possible tools for catalyst evaluation.[15]

In this paper, we present the design and realization of a computerized laboratory batch reactor that can be used as a screening reactor for monopropellant formulations and catalyst evaluation and development. The advantages are 1) easy use, 2) fast change of catalyst or propellant, and 3) very limited consumption of propellant (10–100 μl for one trial) or catalyst (50–200 mg). The first results presented here, concern the decomposition of hydrazine, hydrogen peroxide, and HAN–TEAN–H_2O mixtures.

Experimental Part

Design of the Reactor

This reactor has been build to acquire data on the catalytic ignition reaction of different monopropellants and catalysts at low temperature. The catalyst can be preheated in the 20–250°C range, and two operation modes are achieved: constant temperature mode and temperature increase mode. However, this reactor cannot be used to obtain data relating to real conditions in a satellite thruster.

The reactor is a constant volume batch reactor (168-ml, stainless steel AISI-316L, AFNOR-Z2CND1712) with operating pressure between vacuum and 2 bar. Figure 1 shows the scheme of the reactor facility with the different gauges, and Fig. 2 shows a side and top views with dimensions in millimeters. Three temperature gauges for heating elements, catalyst (item 3, Fig. 1) and inside atmosphere (item 2, Fig. 1), and one pressure gauge (item 1, Fig. 1) are connected to the computer through a Netdaq 2645A interface (Fluke Company, Canada), with three acquisition frequencies, 1 kHz, 400 Hz, and 40 Hz. The temperature gauges are nonprotected, laboratory-welded K thermocouples (chromel–alumel) with low time constant (less than 0.1 s). The pressure gauge (Keller, type PAA-23) displays a time response of less than 1 ms in the range 0–2 bar. The evacuation of the

Presented as Paper 2000-3553 at the AIAA/ASME/SAE/ASEE 36th Joint Propulsion Conference and Exhibit, Huntsville, AL, 17–19 July 2000; received 13 September 2001; revision received 4 October 2002; accepted for publication 21 October 2002.

*Dr., Department of Chemistry; currently Post Doctoral Fellow, Institute of Transuranium Elements, Karlsruhe, Postfach 2340, D-76125, Germany.
†Assistant Professor, Laboratoire de Catalyse en Chimie Organique.
‡Professor, Laboratoire de Catalyse en Chimie Organique, Catalyse par les Métaux, 40 Avenue du Recteur Pineau; Charles.Kappenstein@univ-poitiers.fr. Member AIAA.
§Research Manager, Laboratoire de Catalyse en Chimie Organique.
¶Dipl.-Ing., Propulsion and Pyrotechnic Department, 18 avenue Edouard Belin; Nicolas.Pillet@cnes.fr.

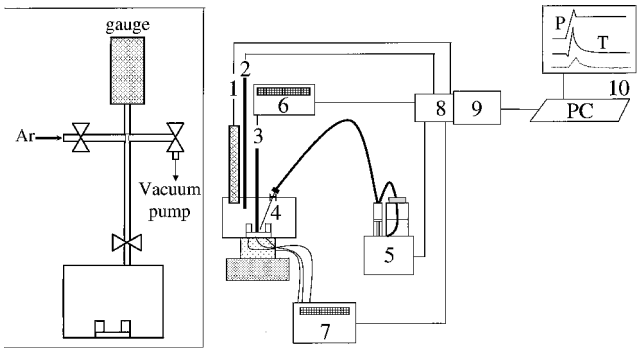

Fig. 1 Scheme of the reactor with the different gauges: 1) pressure gauge; 2) K thermocouple; 3) K thermocouple; 4) needle or syringe; 5) microburette; 6) digital indicator; 7) heat regulator; 8) connection box; 9) interface; and 10) personal computer.

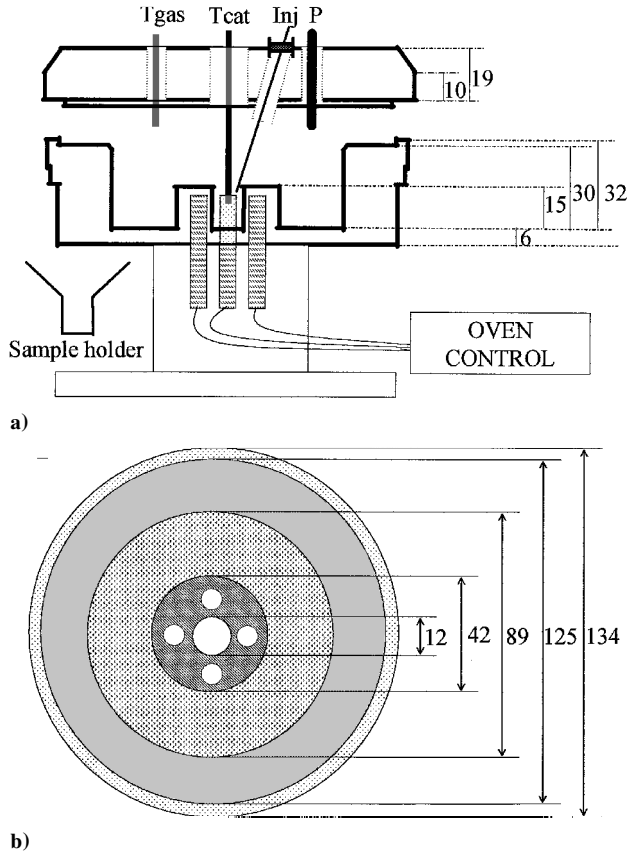

Fig. 2 Reactor: a) side view, where Tgas and Tcat are thermocouples for the gas-phase temperature and the catalyst temperature, Inj is the injection needle through the septum, and P is the pressure gauge and b) top view.

reactor and argon fill are obtained through a vacuum line (Fig. 1), and a second pressure gauge (Pirani type, Edwards Company) controls the quality of the vacuum.

The catalyst (50–200 mg) can be heated with a fixed heating rate or preheated at a defined temperature. It is placed inside a specific sample holder (Fig. 2), which prevents the loss of sample after possible ejections during the exothermic decomposition. The monopropellant is added through a microsyringe (Hamilton, 10 or 100 μl) or by using an automatic burette (Metrohm 765, total volume 1 ml). Between successive monopropellant injections, the decomposition products can be quickly evacuated through the vacuum line up to 10^{-2} mbar. This reactor can be used to simulate cold starts or pulsed injections, but not stationary monopropellant flow (steady-state studies).

Blank experiments without catalyst were performed with hydrogen peroxide and aqueous HAN–TEAN mixture to verify that the sample holder displays no catalytic activity. In the case of the HAN–TEAN–water mixture, the thermal decomposition has shown an ignition temperature in agreement with the literature (shown later). Therefore, no special surface treatment of the sample holder was carried out. No blank experiment has been performed with hydrazine for security reasons.

The mode of operation of this reactor is near isobaric, the pressure increase being a fraction (a few tenths) of the initial pressure. If the catalyst is not preheated, the mode of operation is isothermal due to the high heat capacity of the reactor. The order of magnitude of the heat capacity ratio between reactor and catalyst is about 5000 (2-kg steel, 200-mg catalyst). As an example, the decomposition of 30 μl of hydrazine leads to a final temperature increase for the whole reactor of 0.12°C. The reactor itself is not heated; when the catalyst is preheated at the bottom central part (Fig. 2), the reactor displays a temperature gradient, with the top being near room temperature. The average gas temperature as measured by the thermocouple is lower than the catalyst temperature and is taken into account for the calculations.

For very fast decomposition of the monopropellant, the pressure gauge displays a pressure spike before reaching a plateau corresponding to the equilibrium pressure (Fig. 3). For slow decomposition, the pressure rises smoothly to the plateau value (Figs. 3 and 4). The percentage of propellant decomposition can be determined from the pressure increase.

The temperature profile corresponds always to a peak (Figs. 5 and 6). The strongly exothermic decomposition leads to a rapid temperature increase of the catalyst and gas phase. Then, the thermal transfer to the walls of the reactor associated with the large heat capacity decreases the temperature slowly up to the initial value. This temperature decrease extends about 200 s.

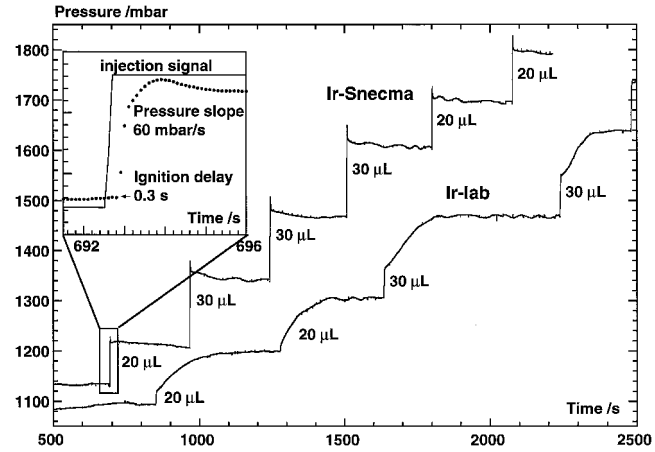

Fig. 3 Comparison of pressure increase vs time for two Ir/Al_2O_3 catalysts after successive hydrazine pulses; enlargement of the first pressure peak (different *x*-axis scale) in inset.

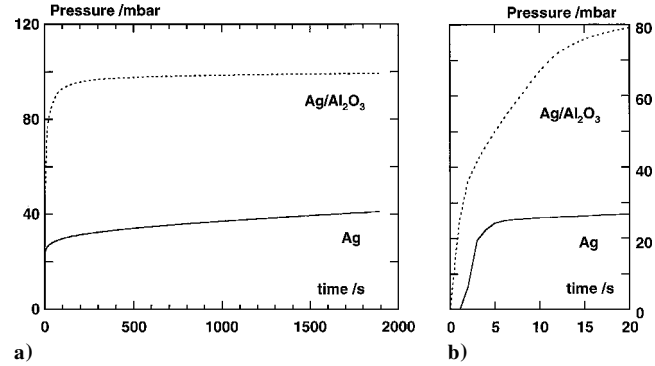

Fig. 4 Decomposition of H_2O_2 vs time on silver catalysts: a) initial temperature 25°C, injection 100-μl H_2O_2 30-wt% in evacuated reactor and b) enlargement of reaction onset.

Table 1 Results of the decomposition of hydrazine at 20°C on two Ir/Al_2O_3 catalysts (200 mg) after successive injections

	Ir-Snecma sample			Ir-lab sample		
N_2H_4 pulse, μl	Pressure increase, mbar	Slope, mbar · s^{-1}	Ignition delay, s	Pressure increase, mbar	Slope, mbar · s^{-1}	Ignition delay, s
20[a]	88	57	0.3	104	8	1.0
20	90	60	0.3	106	5	0.6
30[b]	151	92	0.3	162	18	0.7
30	136	110	0.2	168	27	0.6
30	153	119	0.2	163	22	0.7
20	103	159	0.3	105	23	0.7
20	100	154	0.3	(no injection)		

[a]Calculated pressure increase 98 mbar (formation of ammonia only).
[b]Calculated pressure increase 147 mbar.

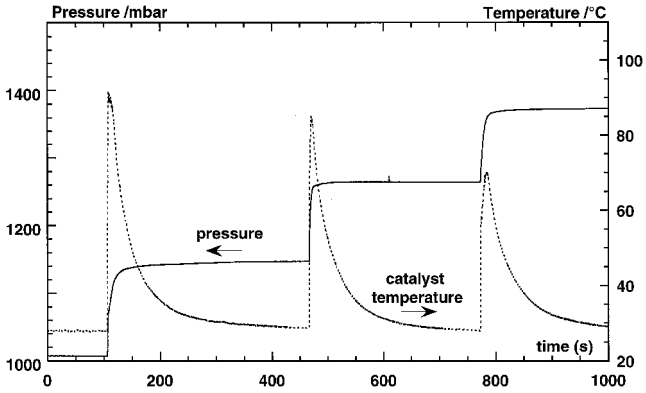

Fig. 5 Decomposition of 50% H_2O_2 on Ag/Al_2O_3 catalyst; variation of pressure and temperature of the catalyst for three successive 100-μl injections from 1-bar argon pressure.

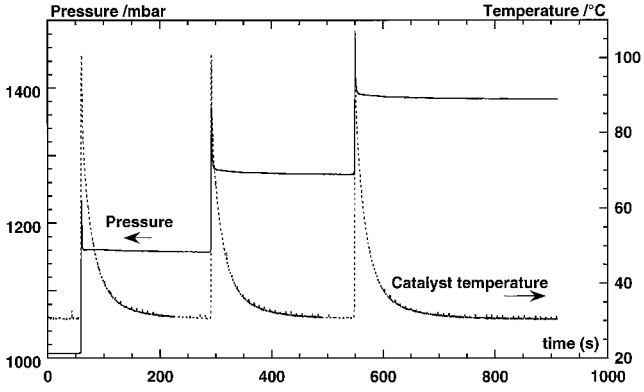

Fig. 6 Decomposition of 50% H_2O_2 on MnO_x/Al_2O_3 catalyst; variation of the catalyst for three successive 100 μL injections from 1 bar argon pressure: ——, pressure and . . . . , temperature.

Monopropellants

Three monopropellants have been used: 1) hydrazine N_2H_4, high purity, supplied by the SNECMA Company, density at 20°C = 1.01 g · cm^{-3}; 2) hydrogen peroxide H_2O_2, 30-wt%, density at 20°C = 1.11 g · cm^{-3}, and 50-wt%, density at 20°C=1.19 g · cm^{-3} (Prolabo, France); and 3) HAN–TEAN–H_2O stoichiometric mixture (7/1 HAN/TEAN), 20-wt% water, equivalent to liquid gun propellant (LGP) 1846 (Ref. 16) (prepared by Cohen-Adad, University of Lyon, France), density = 1.43 g · cm^{-3}.

The HAN [= $(NH_3OH)(NO_3)$] was prepared from hydroxylamine and nitric acid, both of high purity. The TEAN [= $[HN(C_2H_4OH)_3](NO_3)$] was prepared from the corresponding amine and nitric acid, both of high purity.

Catalysts

For N_2H_4 decomposition, the 36-wt% Ir/Al_2O_3 catalysts were supplied by the SNECMA Company (sample Ir-Snecma) and prepared in the laboratory by three successive impregnation and reduction steps (sample Ir-lab).[17]

For H_2O_2 decomposition, the silver or manganese oxide catalysts were Ag (Alfa-Johnson Matthey, 99.99% purity, 10–20 mesh), Ag/α–Al_2O_3 (Strem Chemical, 2-mm-diam spheres, 3.5–4% Ag, Brunauer, Emmett, and Teller isotherm (BET) surface area $S_{BET} = 8\ m^2 \cdot g^{-1}$), and MnO_x/γ–Al_2O_3 powder, prepared by impregnation of the support with $HMnO_4$ followed by calcination at 150°C for 5 h, with no x-ray detectable manganese oxide bulk phase,[18] 1.6-wt% Mn, $S_{BET} = 54\ m^2 \cdot g^{-1}$.

For the HAN–TEAN–H_2O redox decomposition reaction, there were platinum-, rhodium-, or palladium-supported catalysts.

Different supports have been prepared using slow jellification of a colloidal solution processes to improve the thermal stability at very high temperatures through the addition of different doping elements.[19] The precursors of the active phase ($H_2PtCl_6 \cdot nH_2O$, $RhCl_3 \cdot nH_2O$, and $PdCl_2$) are introduced in the porosity of the support through classical impregnation procedures using aqueous solutions.

Results

Decomposition of N_2H_4

The decomposition of hydrazine has been followed to obtain reference values. On supported Ir/Al_2O_3 catalysts, the decomposition of hydrazine at low temperature leads only to the formation of nitrogen and ammonia[20]:

$$3N_2H_4(g) \rightarrow 4NH_3(g) + N_2(g)$$

Two series of pulses, corresponding to the injection of 20 or 30 μl, were carried out at 20°C on both catalysts Ir-lab and Ir-Snecma (200 mg). The first series of hydrazine injections leads to similar results of pressure increase and pressure slope for each injection (not given). The results of the second series of successive injections are listed in Table 1 and presented in Fig. 3 for both catalysts. Drastic differences can be observed: the industrial sample, Ir-Snecma, demonstrates good catalytic activity with very sharp pressure peaks accompanying each step, whereas the laboratory sample, Ir-lab, exhibits a loss of activity as shown by the bad step profiles (Fig. 3); nevertheless, the final pressure increases are the same for both catalysts and depend only on the volume of the injection. The experimental values are in agreement with the values calculated on the basis of the preceding equation (Table 1).

For the Ir-Snecma sample, the ignition delay is of the order 0.2–0.3 s (first injection, inset in Fig. 3) and is related to the time needed for the liquid to be adsorbed into the porosity of the catalyst support. The pressure slope ranges from 50 to 160 mbar · s^{-1} and increases with the number of pulses (Table 1), which means that the surface of the catalyst is reactivated under the reductive atmosphere of the reaction products. The pressure maximum is reached in less than 1 s. For a 30-μl pulse, the molar ratio (N_2H_4)/(surface Ir) is 13, when a metal dispersion of 20% is assumed; therefore, each surface

Table 2 Decomposition of 30-wt% H_2O_2 on two silver catalysts (200 mg)[a]

Trial	Initial temperature, °C	Initial pressure, mbar	Final pressure, mbar	ΔP_{exp}, mbar	ΔP_{calc}, mbar
		Ag			
A	25	$<10^{-2}$	>100	>100	104[b]
		Ag/Al_2O_3			
B	25	$<10^{-2}$	>100	>100	104[b]
C	25	1020	1088	68	72
D	50	$<10^{-2}$	>180	>180	201[b]

[a]Injection of 100 μl in evacuated reactor or at atmospheric pressure.
[b]Including the vapor pressure of water, 32 mbar at 25°C and 123 mbar at 50°C.

Table 3 Decomposition of 50% H_2O_2[a]

Injection number	Pressure increase, mbar	Pressure slope, mbar · s^{-1}	Initial T, °C	T_{max} catalyst, °C	T_{max} gas phase, °C
		Ag/Al_2O_3			
1	138[b]	47	28	91	29
2	117	36	28	85	29
3	108	24	28	70	29
		MnO_x/Al_2O_3			
1	152[b]	170	30	101	50
2	121	196	30	102	50
3	118	212	30	103	48

[a]Successive pulses of 100 μl on two catalyst samples (200 mg).
[b]Including the vapor pressure of water (38 mbar at 28°C and 42 mbar at 30°C).

iridium atom has to participate in the decomposition of an average value of 13 hydrazine molecules.

The Ir-lab catalyst shows stepped pressure increases followed by rounded pressure profiles. For the step parts, the slopes are much lower than for the Ir-Snecma sample (between 5 and 27 mbar s^{-1}), and the ignition delays are more pronounced (0.6–1.0 s, Table 1). This lower activity can be explained by a poisonous effect of ammonia on this sample.

In conclusion, the difference in catalytic activity between the two supported iridium catalysts is clearly evidenced through the use of the batch reactor. Further studies concerning the variation of the catalytic activity, the poisonous role of ammonia, and the relations to structural and textural parameters are currently under investigation.

Decomposition of H_2O_2

30% H_2O_2

Two commercial silver catalysts were compared at 25°C: grain silver (low metallic surface area) and alumina-supported silver Ag/Al_2O_3 (high metallic surface area). Table 2 gives a part of the results obtained, and Fig. 4 shows a comparison of both catalysts. As expected, the decomposition reaction starts at room temperature:

$$H_2O_2(aq) \rightarrow H_2O(g) + \tfrac{1}{2}O_2(g)$$

The activity of the supported catalyst is much higher by comparison with pure silver, and this can be obviously related to the higher specific surface area. The decomposition rate, as measured by the pressure increase, is rapid at the onset of the reaction. In the range 0–6 s, the average slopes are 9.6 and 6.5 mbar · s^{-1} and the decomposition delay is less than 1 and 2 s, respectively, for the supported and the unsupported catalysts (Fig. 4b). After 10 s, the activity decreases strongly, which leads to an approximately constant rate: 0.24 mbar · s^{-1} for Ag/Al_2O_3 and 0.07 mbar · s^{-1} for Ag in the range 10–20 s.

The pressure increase due to the evolved oxygen after 100 s is three time higher for the supported catalyst, approaching the calculated value for a whole decomposition (91 vs 102 mbar, Fig. 4a). Note that this final pressure value includes the vapor pressure of water. After sufficient time (2000 s for supported catalyst vs 20,000 s for unsupported silver), the pressure increase reaches the calculated value in an asymptotic way (Table 2).

50% H_2O_2

Figures 5 and 6 show the results obtained on two alumina-supported catalysts containing silver or manganese oxide as the active phase. The initial pressure is about 1-bar argon, and the catalyst mass is 200 mg. Three successive injections (100 μl) are performed on the catalyst preheated at about 30°C. The reactor pressure, the temperature of the catalyst, and the temperature of the gaseous atmosphere (not shown) have been simultaneously recorded, and the corresponding data are given on Table 3.

For both catalysts, the pressure steps correspond exactly to the temperature peaks, and the expanded view presented in Fig. 7 shows that the temperature variations of the catalyst and the gas phase follow very well the pressure changes at the time level of 0.1 s, in accordance with the short response time of the thermocouple gauges; therefore they display the same decomposition delay (about 0.3 s for this case).

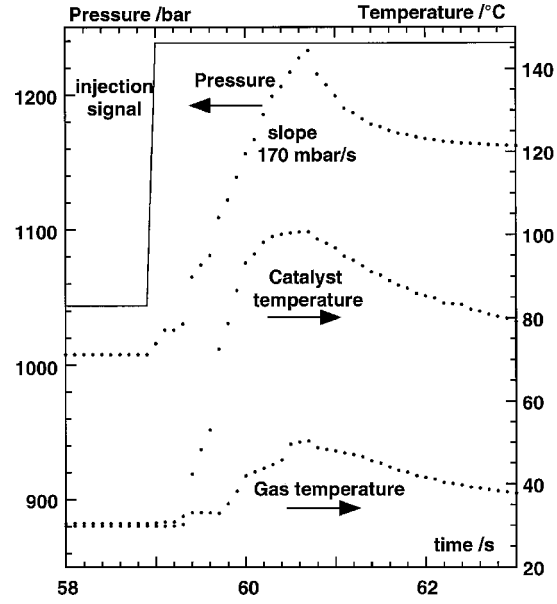

Fig. 7 Expanded view of the first pulse of Fig. 6; data frequency is 10 s^{-1} for each gauge.

Comparison of Figs. 5 and 6 shows different pressure profiles; the manganese oxide-based sample displays better activity with sharp pressure peaks before the pressure steps and thinner temperature peaks. The first pressure increase is higher than the following ones because it includes the water vapor pressure corresponding to the liquid–vapor equilibrium. For the three injections, the temperature maximum corresponds to a small plateau at 101–103°C lasting about 0.5 s in full agreement with the vaporization of a part of the water. (See the catalyst temperature in Fig. 6 or 7 and Table 3.) The pressure slope is of the order of 200 mbar · s^{-1} and increases slightly with the injection number.

The supported silver sample is less active and shows a slight loss of activity evidenced by the decrease of the pressure slope from 47 to 24 mbar · s^{-1}, the decrease of the maximal temperature of the catalysts from 91 to 70°C, and the lower maximum temperature reached by the gas (29 vs 50°C for the manganese oxide catalyst, Table 3). Therefore, it is possible to discriminate easily between various types of catalysts. In our case, the difference in activity can be related to the different surface area (8 and 54 $m^2 \cdot g^{-1}$) and to the catalyst shape (spheres and powder).

Decomposition of HAN–TEAN–H_2O mixture (LGP 1846)

Different parameters can be analyzed by using the batch reactor, such as the initial pressure (vacuum or atmospheric pressure), the

Table 4 Decomposition of HAN–TEAN–H_2O mixtures (LGP 1846)[a]

Trial number	Volume, μl	ΔP_{exp}, mbar	ΔP_{calc}, mbar	T_{ini},[b] °C	T_{max},[c] °C	ΔT,[d] °C
		Thermal decomposition				
1	50	72	146	117	173	56
2	50	85	142	106	164	58
3	50	82	141	97	147	50
		Catalytic decomposition (catalyst B4151)				
4	30	62	87	74	124	50
5	50	108	146	66	158	92
6	40	85	117	74	121	47
7	50	98	146	75	124	49

[a] Reactor evacuated after each injection.
[b] Onset temperature of decomposition.
[c] Maximal temperature.
[d] $(T_{max} - T_{ini})$.

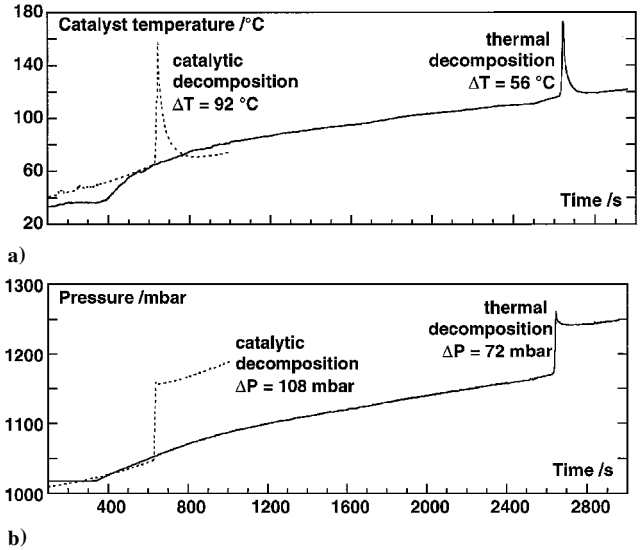

Fig. 8 Thermal decomposition (trial 1, Table 4) and catalytic decomposition (trial 5, Table 4) of HAN–TEAN–H_2O monopropellant mixture (50 μl of LGP 1846); variation of a) sample temperature and b) reactor pressure vs time during temperature increase.

amount of injected monopropellant, and the nature and amount of catalyst sample.

The batch reactor can be used in two modes: 1) temperature increase mode (1–5°C · min^{-1}) mainly to determine the onset temperature of decomposition and 2) the constant temperature mode (between room temperature and 250°C). When the second mode is used, it is possible to make successive monopropellant injections with or without intermediate gas evacuation, to simulate the cold start conditions.

Temperature Increase Mode

Figure 8 shows typical curves of the variation of sample temperature (Fig. 8a) and reactor pressure (Fig. 8b) during heating in the case of the thermal decomposition (no catalyst in the sample holder) or catalytic decomposition. Table 4 gives a part of the results.

The thermal decomposition begins at 117°C for the first trial (Fig. 8a), in agreement with literature data (122°C in Ref. 21). The full decomposition of LGP 1846 into water, carbon dioxide, and nitrogen corresponds to the following equation:

$$7NH_3OHNO_3(aq) + NH(C_2H_4OH)_3NO_3(aq)$$
$$\rightarrow 22H_2O(g) + 8N_2(g) + 6\,CO_2(g)$$

This leads to a calculated pressure increase higher than the observed value in our conditions (Table 4). Therefore, the decomposition into gaseous products is not complete, and in fact a yellow brownish carbonaceous residue was present in the reactor, probably due to a polymerization reaction of the C_2H_4 fragments of TEAN. Curiously, this residue, once obtained seems to affect the subsequent trials because we can observe a decrease of the onset temperature decomposition (Table 4) and a slight pressure increase. Therefore, without the presence of a catalyst, the thermal decomposition reaction can lead to thermodynamic gaseous products, as expected by the preceding equation, and to more condensed kinetic products resulting from polymerization reactions. An elemental analysis of these products is presently under study.

In the presence of a supported noble metal catalyst (catalyst B4151), the onset of the decomposition is much lower (about 70°C in Table 4 for several trials; 66°C for trial 5 shown in Fig. 8a) thus disclosing the real catalytic effect. The corresponding pressure increase is higher than the value obtained during the thermal decomposition (Fig. 8b), which showed that the formation of polymerized products remains more limited in the case of the catalytic decomposition (Table 4).

After numerous trials, we observed that the decomposition of LGP1846 is very sensitive to the rate of temperature increase, the nature of the crucible, and the amount of reactant. The different experiments performed by means of the batch reactor raise the following points.

1) All samples display a catalytic effect on LGP 1846 decomposition by decreasing the onset temperature.

2) The yield never reaches 100%.

3) The resulting carbonaceous residue has a catalytic effect.

Constant Temperature Mode

Two typical results are presented in Figs. 9 and 10. In Fig. 9, the catalyst sample (A1151) was preheated at 92°C. The injection of 50 μL of LGP (at 20°C) leads first to a 10°C decrease of the catalyst temperature due to the temperature difference between catalyst and monopropellant. Then the temperature slowly rises up to the start of the decomposition. During the same time, the pressure increases slowly at a rate of 0.29 mbar · s^{-1} due to the vaporization of the water part of the monopropellant. After a rather long ignition delay (49 s),

Table 5 Pressure increase in mbar after an injection of 50 μl of LGP at 90 and 130°C for different catalysts

Catalysts	ΔP_{exp}, mbar						Calculated,[a]
T_{cata},[b] °C	A1151	F1151	B4151	A4151oxid	C4151	4151	mbar
90	154	147	175	151	162	134	268
130	223	269	290	260	266	192	299

[a] Calculated values take into account the formation of CO_2(g), N_2(g) and H_2O(g) corresponding to the liquid–vapor equilibrium.
[b] Temperature of the catalyst.

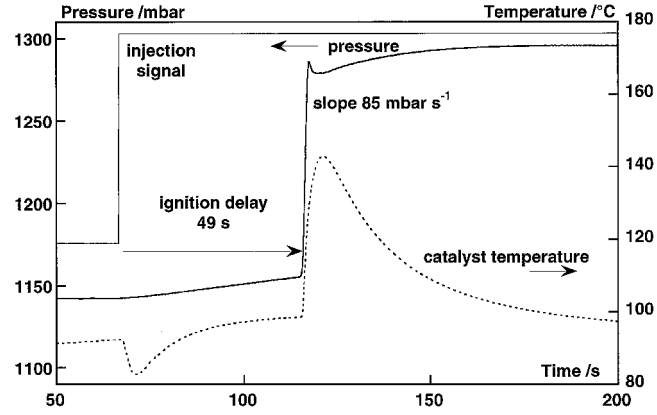

Fig. 9 Pressure and temperature variations vs time after a pulse of 50 μl of LGP at 92°C on 200 mg of catalyst A1151.

Table 6 Best values obtained

Parameter	Propellant (associated catalyst)		
	N_2H_4 (Ir/Al_2O_3)	H_2O_2 (MnO_x/Al_2O_3)	LGP 1846 (A1151)
Initial temperature, °C	20	30	130
Rate, mbar · s^{-1}	159	212	152
Ignition delay, s	0.2	0.3	0.6

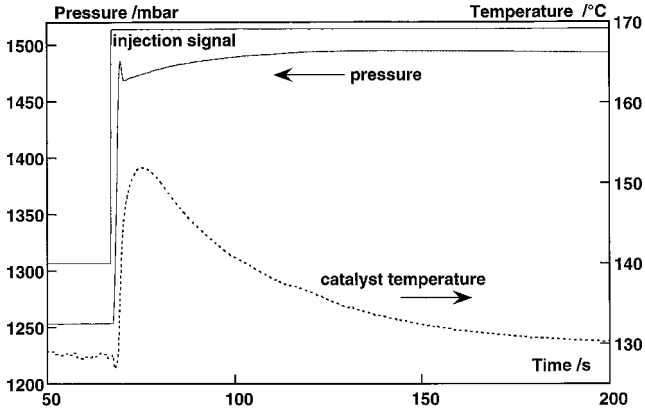

Fig. 10a Pressure and temperature variations vs time after a pulse of 50 μl of LGP at 130°C on 200 mg of catalyst A1151 (same time scale as Fig. 9).

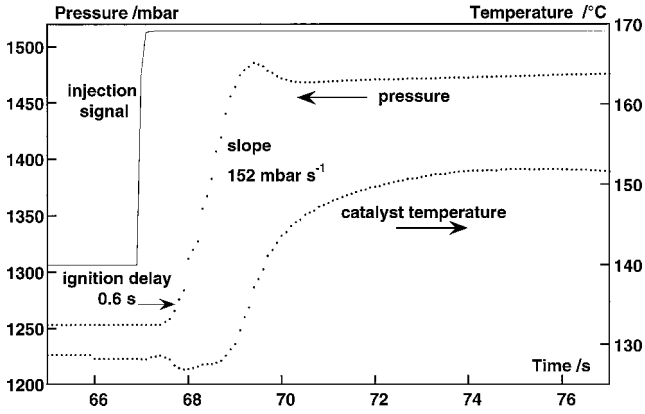

Fig. 10b Expanded view of the pressure and temperature peaks (note expanded *x* scale).

we can observe the simultaneous step increases of temperature (up to 143°C) and pressure with a rate of 85 mbar · s^{-1} (Fig. 9).

Figure 10a shows the results obtained with the same catalyst but for a higher initial temperature (130°C); Fig. 10b is an expanded view of Fig. 10a. The pressure and temperature profiles are the same, and the main difference is the much shorter ignition delay (0.6 s, Fig. 10b). The rate is about twice the earlier value (152 mbar · s^{-1}), and the pressure increase is higher (223 mbar vs 154 mbar at 90°C). The results of pressure increase for different catalyst samples are gathered in Table 5. A support without an active phase (sample 4151) presents an intrinsic catalytic activity, but with a lower pressure increase (and generally a higher onset temperature), by comparison with the samples including an active phase. The differences are more pronounced at 130°C than at 90°C (Table 5).

Table 6 compares the best values obtained for the three propellants under study and their associated catalysts. The activities as measured by the rate of pressure increase and the ignition delay are of the same order of magnitude. Other catalysts and monopropellant compositions are currently under investigation.

Conclusions

The batch reactor has fulfilled our objectives and will be able to be used as a screening reactor for different catalysts, as well as for different monopropellant compositions. The catalysts are easily evaluated and compared with the same propellant, and the samples can be ordered from their catalytic activity. In the case of the HAN-based propellant, the presence of CH_2–CH_2 fragments in the fuel component of the propellant could be a drawback for a full decomposition into gaseous products.

This laboratory reactor is an efficient tool to evaluate the catalytic activity related to the ignition of the monopropellant (cold starts or pulse injections). Once the reaction is started, the role of the catalytic bed is to assume good combustion without degradation of the support or active phase at the very high temperature obtained. However, in the end, this evaluation has to be performed by using a dynamic reactor.

Acknowledgments

We thank the French Space Agency, Centre National d'Etudes Spatiales, Toulouse, for funding this study, S. Fouché and A. Melchior (SNECMA) for helpful discussions, M. T. Cohen-Adad and R. Cohen-Adad (University of Lyon) for the preparation of the hydroxylammoniumnitrate–triethanolammoniumnitrate–water mixtures, and M. Chauveau (Chemistry Dept., Poitiers) for the realization of the reactor.

References

[1]Schmidt, E. W., "Hydrazine Application," *Hydrazine and Its Derivatives. Preparation, Properties, Applications*, 2nd ed., Wiley, New York, 2001, pp. 1267–1474.

[2]Jankowsky, R. S., "HAN-Based Monopropellant Assessment for Spacecraft," AIAA Paper 96-2863, July 1996.

[3]Callahan, L. W., Curran, F. M., and Wickenheiser, T. J., "Onboard Propulsion for Communications Satellites," AIAA Paper 96-1142, Feb. 1996.

[4]Morgan, O. M., and Meinhardt, D. S., "Monopropellant Selection Criteria: Hydrazine and Other Options," AIAA Paper 99-2595, June 1999.

[5]Mittendorf, D., Facinelli, W., and Sarpolus, R., "Experimental Development of a Monopropellant for Space Propulsion Systems," AIAA Paper 97-2951, July 1997.

[6]Meinhardt, D., Brewster, G., Christofferson, S., and Wucherer, E. J., "Development and Testing of New HAN-Based Monopropellants in Small Rocket Thrusters," AIAA Paper 98-4006, July 1998.

[7]Meinhardt, D. S., Wucherer, E. J., Jankovsky, R. S., and Schmidt, E. W., "Selection of Alternate Fuels for Han-Based Monopropellants," *JANNAF Propellant Development and Characterization Subcommittee and Safety and Environmental Protection Subcommittee Joint Meeting*, CPIA Publication, Vol. 1, 1998, pp. 143–151.

[8]Meinhardt, D., Christofferson, S., and Wucherer, E. J., "Performance and Life Testing of Small HAN Thrusters," AIAA Paper 99-2881, June 1999.

[9]Rusek, J., "New Decomposition Catalysts and Characterization Techniques for Rocket-Grade Hydrogen Peroxide," *Journal of Propulsion and Power*, Vol. 12, No. 3, 1996, pp. 574–579.

[10]Wernimont, E. J., and Mullens, P., "Recent Developments in Hydrogen Peroxide Monopropellant Devices," AIAA Paper 99-2741, June 1999.

[11]Wernimont, E. J., and Meyer, S. E., "Hydrogen Peroxide Hybrid Rocket Engine Performance Investigation," AIAA Paper 94-3147, July 1994.

[12]Wernimont, E., and Garboden, G., "Experimentation with Hydrogen Peroxide Oxidized Rockets," AIAA Paper 99-2743, June 1999.

[13]Ventura, M., and Mullens, P., "The Use of Hydrogen Peroxide for Propulsion and Power," AIAA Paper 99-2880, June 1999.

[14]Morlan, P., Wu, P., Nejad, A., Ruttle, D., and Fuller, R., "Catalyst Development for Hydrogen Peroxide Rocket Engines," AIAA Paper 99-2740, June 1999.

[15]Christofferson, S., Wucherer, E. J., and Zube, D. M., "Tools for Monopropellant Catalyst Development," AIAA Paper 01-3941, July 2001.

[16]Klingenberg, G., Knapton, J. D., Morrison, W. F., and Wren, G. P., "Liquid Propellants," *Liquid Propellant Gun Technology*, Vol. 175, Progress in Astronautics and Aeronautics, AIAA, Reston, VA, 1997, pp. 81–118.

[17]Mary, S., Kappenstein, C., Balcon, S., Rossignol, S., and Gengembre, E., "Monopropellant Decomposition Catalysts. I. Ageing of Highly Loaded Ir/Al2O3 Catalysts in Oxygen and Steam. Influence of Chloride Content," *Applied Catalysis A: General*, Vol. 182, No. 2, 1999, pp. 317–325.

[18]Kappenstein, C., Wahdan, T., Duprez, D., Zaki, M. I., Brands, D., Poels, E., and Bliek, A., "Permanganic Acid: A Novel Precursor for the Preparation of Manganese Oxide Catalysts," *Studies in Surface Science and Catalysis*, Elsevier, Amsterdam, Vol. 91, 1995, pp. 699–706.

[19]Rossignol, S., and Kappenstein, C., "Effect of Doping Elements on the Thermal Stability of Transition Alumina," *International Journal of Inorganic Materials*, Vol. 3, No. 4, 2001, pp. 51–58.

[20]Balcon, S., "Préparation, Caractérisation et Activité en Décomposition de l'Hydrazine de Catalyseurs Supportés Ir/Al2O3. Contrôle de la Taille des Particules Métalliques," Ph.D. Dissertation, Dept. of Chemistry, Univ. of Poitiers, Poitiers, France, Nov. 1996.

[21]Klein, N., and Leveritt, C. S., "Methods for Evaluation of Thermally Induced Reactions in Liquid Propellants," Rept. BRL-TR-3069, 1989, Order AD-A218750, National Technical Information Service, U.S.